

## ***2. Elastic Buckling Solution Methods for Cold-Formed Steel Elements and Members***

Cold-formed steel elements and members are often quite slender. it is not uncommon for elastic buckling stresses to be much lower than the material yield stress. Therefore, buckling often dominates the behavior. Although elastic buckling does not fully describe the ultimate behavior it can be an important part of characterizing that behavior. Careful definitions of elastic buckling shall be left to others, here an engineering approach is taken: elastic buckling refers to the determination of a load in which the member is in equilibrium both in a straight and slightly bent configuration. Such a loading and the corresponding bent configuration, form the buckling load (stress) and buckling mode for the member.

Calculation of the elastic buckling stress and modes can be completed in a variety of ways. Three common methods: finite element analysis, finite strip analysis, and classical Fourier Series solutions are presented here. These techniques are by no means the only possible solution methods. For example, infrequently used techniques such as the boundary element method can be employed successfully (Elzein 1991).

Presentation of the finite element, finite strip, and Fourier Series methods are given in detail because these methods are used throughout this work, and each have their own particular advantages. Elastic buckling calculations via the finite element method are advantageous for unusual geometry or varying boundary conditions along the length. In addition, the finite element elastic buckling solution is a useful tool for generating imperfection configurations when more general nonlinear analysis is to be performed. The finite strip method allows for an efficient solution of problems which may have complex geometry in their cross-section, but are simple along the length. The finite strip method lends itself to parameter studies due to its simple requirements on input and the speed of the solution. The classical Fourier Series solutions are useful because they have the potential to yield closed-form solutions, which are advantageous for design approximations.

### **2.1 FINITE ELEMENT ANALYSIS**

{section removed in this excerpt}

## 2.2 FINITE STRIP ANALYSIS

The finite strip method was originally developed by Y.K. Cheung. An excellent summary of the method, and the theory behind it, can be found in his book (Cheung 1976). The use of the finite strip method for understanding and predicting the behavior of hot-rolled steel members, and cold-formed steel members has been greatly extended by G. Hancock. Hancock used the stiffness matrices derived in Cheung's book, and with some modification, created BFINST - a computer program for solution of the elastic buckling problem of open thin-walled members via finite strip. His early work in the field on I-Beams (Hancock 1977, 1978) led to the acceptance and understanding of the use of the finite strip method. More recently, in a book on cold-formed steel design, the use of the finite strip method as a design aid is explicitly shown (Hancock 1994).

Finite strip analysis provides a convenient and efficient way to determine the elastic buckling stress and corresponding modes. In this section, an introduction to the basic differences between the finite element method and the finite strip method is provided. This is followed by the initial stiffness and geometric stiffness matrices for a finite strip. These matrices are presented in their entirety because they are employed in a program written by the author. Details of the program (CUSTRIP) and verification problems can be found in the Appendix.

### 2.2.1 Introduction and Comparison to Finite Element Method

The finite strip method can be considered as a specialization of the finite element method. The basic methodology and theory of the two methods is identical. Shape functions are used to define the displacement field in terms of nodal degrees of freedom. Strain is defined in terms of the nodal degrees of freedom, since strain is a function of the displacement field. With strain defined, and a constitutive relationship known, (i.e., the stress-strain relationship) stiffness coefficients for the nodal degrees of freedom can be derived.

The only difference between the finite element and finite strip methods is the discretization of a member. The finite strip method, is so named, because only a single element (strip) is used to model the longitudinal direction. The result of the differing discretization assumptions are depicted in Figure 2.1.

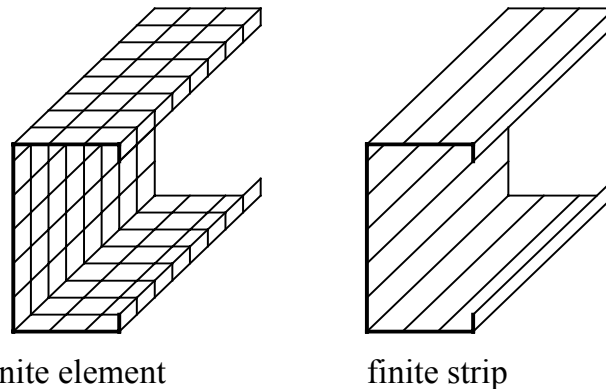


Figure 2.1 Finite Element and Finite Strip Discretization

The advantages and accuracy of the finite strip solution is dependent on a judicious choice of the shape function for the longitudinal displacement field. Using the finite strip method, the total number of equations needed for the solution are greatly reduced from that of a typical finite element solution.

### 2.2.2 Initial Stiffness Matrix for Plates

The stiffness matrix presented in this section follows directly from the work presented by Cheung (1976). The presentation here is also similar to the work of Hancock (1977) and Mulligan (1983). The strip (element) and its degrees of freedom are shown in Figure 2.2.

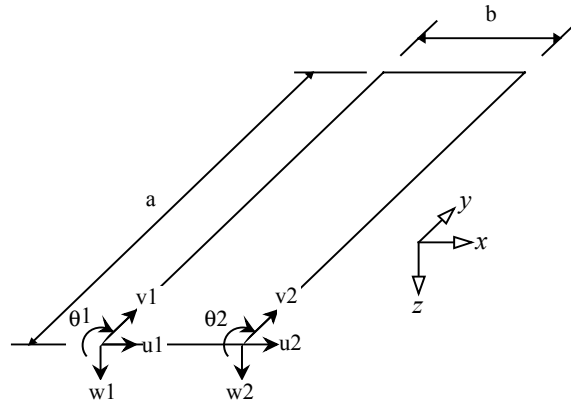


Figure 2.2 Strip, Degrees of Freedom

The standard definition of an initial stiffness matrix is apparent from:

$$\{F\} = [K]\{d\}$$

or, expanded to explicitly show the nodal forces, nodal degrees of freedom, and the initial stiffness submatrices:  $[K_{uv}]$  (plane stress) and  $[K_{w\theta}]$  (bending):

$$\begin{Bmatrix} F_{u_1} \\ F_{v_1} \\ F_{u_2} \\ F_{v_2} \\ F_{w_1} \\ M_{\theta_1} \\ F_{w_2} \\ M_{\theta_2} \end{Bmatrix} = \begin{bmatrix} & & & & 0 & 0 & 0 & 0 \\ & [K_{uv}] & & & 0 & 0 & 0 & 0 \\ & & & & 0 & 0 & 0 & 0 \\ & & & & 0 & 0 & 0 & 0 \\ 0 & 0 & 0 & 0 & & & & \\ 0 & 0 & 0 & 0 & & [K_{w\theta}] & & \\ 0 & 0 & 0 & 0 & & & & \\ 0 & 0 & 0 & 0 & & & & \end{bmatrix} \begin{Bmatrix} u_1 \\ v_1 \\ u_2 \\ v_2 \\ w_1 \\ \theta_1 \\ w_2 \\ \theta_2 \end{Bmatrix}$$

The initial stiffness matrix may be expressed as:

$$[K] = \int [B]^T [E] [B] dV \text{ or } \int [N']^T [E] [N'] dV$$

Where:  $[B]$  or  $[N']$  is the appropriate derivatives of the shape functions  $[N]$ .  $[N]$ , the shape function, is defined from  $(u \ v \ w)^T = [N] \{d\}$ . Where,  $(u \ v \ w)^T$  is the displacement field and  $\{d\}$  is a vector of the nodal degrees of freedom.

For an orthotropic plate, and assuming no variation in the thickness ( $t$ ) of the strip,  $[K]$  may be expressed as:

$$[K] = t \int [B]^T [D] [B] dA$$

The plate rigidities are defined as:

$$[D] = \begin{bmatrix} D_x & D_1 & 0 \\ D_1 & D_y & 0 \\ 0 & 0 & D_{xy} \end{bmatrix}$$

$$D_x = \frac{E_x t^3}{12(1 - \nu_x \nu_y)} \quad D_y = \frac{E_y t^3}{12(1 - \nu_x \nu_y)}$$

$$D_{xy} = \frac{G t^3}{12} \quad D_1 = \frac{\nu_y E_x t^3}{12(1 - \nu_x \nu_y)} = \frac{\nu_x E_y t^3}{12(1 - \nu_x \nu_y)}$$

As mentioned before, the key to the finite strip method is the selection of the shape functions  $[N]$ . The finite strip solution used here employs a polynomial in the transverse direction and a harmonic function in the longitudinal direction. In this derivation, the longitudinal direction is assumed to take the form of a half sine wave. This is consistent with the **boundary condition of simply supported ends**. The advantage of such an assumption is that the integrals used in forming the stiffness matrix decouple, and the solution is simplified. Other boundary conditions result in far more complex stiffness matrices, see Cheung (1976).

The derivation of the initial stiffness matrix is in two completely decoupled parts. A pure plane stress condition is assumed for the in plane  $u$  and  $v$  degrees of freedom. The  $w$  and  $\theta$  degrees of freedom are derived using classical small deflection plate theory to arrive at the bending initial stiffness matrix. The two matrices  $[K_{uv}]$  and  $[K_{w\theta}]$  are combined to form the total initial stiffness matrix.

### 2.2.2.1 Plane Stress Initial Stiffness Matrix $[K_{uv}]$

The shape functions for use in determining the in plane stiffness matrix are:

$$u = \left[ \left( 1 - \frac{x}{b} \right) \quad \left( \frac{x}{b} \right) \right] \begin{Bmatrix} u_1 \\ u_2 \end{Bmatrix} Y_m \quad v = \left[ \left( 1 - \frac{x}{b} \right) \quad \left( \frac{x}{b} \right) \right] \begin{Bmatrix} v_1 \\ v_2 \end{Bmatrix} \frac{a}{m\pi} Y_m$$

$$Y_m = \sin\left(\frac{m\pi y}{a}\right)$$

The expressions can be put in the general form  $[N]$  such that:

$$\begin{Bmatrix} u \\ v \end{Bmatrix} = [N] \begin{Bmatrix} u_1 \\ v_1 \\ u_2 \\ v_2 \end{Bmatrix} = [N] \{d\}$$

With the shape functions in this form, the strain-displacement matrix  $[B]$  can be written in terms of derivatives of  $[N]$ :

$$\begin{Bmatrix} \varepsilon_x \\ \varepsilon_y \\ \gamma_{xy} \end{Bmatrix} = \begin{Bmatrix} \partial u / \partial x \\ \partial v / \partial y \\ \partial u / \partial y + \partial v / \partial x \end{Bmatrix} = [B] \{d\} = [N'] \{d\}$$

Using these definitions, and performing the necessary substitutions in to the expression for the stiffness matrix presented before, the explicit plane stress stiffness matrix for an element, or strip is given in Figure 2.3.



$$[K_{w\theta}] = \begin{bmatrix} \left( \frac{13ab}{70} k_m^4 D_y + \frac{12a}{5b} k_m^2 D_{xy} + \frac{6a}{5b} k_m^2 D_1 + \frac{6a}{b^3} D_x \right) & \left( \frac{ab^3}{210} k_m^4 D_y + \frac{4ab}{15} k_m^2 D_{xy} + \frac{2ab}{15} k_m^2 D_1 + \frac{2a}{b} D_x \right) & \left( \frac{13ab}{70} k_m^4 D_y + \frac{12a}{5b} k_m^2 D_{xy} + \frac{6a}{5b} k_m^2 D_1 + \frac{6a}{b^3} D_x \right) & \left( \frac{ab^3}{210} k_m^4 D_y + \frac{4ab}{15} k_m^2 D_{xy} + \frac{2ab}{15} k_m^2 D_1 + \frac{2a}{b} D_x \right) \\ \left( \frac{3a}{5} k_m^2 D_1 + \frac{a}{5} k_m^2 D_{xy} + \frac{3a}{b^2} D_x + \frac{11ab^2}{420} k_m^4 D_y \right) & \left( \frac{13ab^2}{840} k_m^4 D_y - \frac{a}{5} k_m^2 D_{xy} - \frac{a}{10} k_m^2 D_1 - \frac{3a}{b^2} D_x \right) & \left( \frac{13ab^2}{840} k_m^4 D_y - \frac{a}{5} k_m^2 D_{xy} - \frac{a}{10} k_m^2 D_1 - \frac{3a}{b^2} D_x \right) & \left( \frac{ab^3}{210} k_m^4 D_y + \frac{4ab}{15} k_m^2 D_{xy} + \frac{2ab}{15} k_m^2 D_1 + \frac{2a}{b} D_x \right) \\ \left( \frac{9ab}{140} k_m^4 D_y - \frac{12a}{5b} k_m^2 D_{xy} - \frac{6a}{5b} k_m^2 D_1 - \frac{6a}{b^3} D_x \right) & \left( \frac{3ab^3}{840} k_m^4 D_y - \frac{ab}{15} k_m^2 D_{xy} - \frac{ab}{30} k_m^2 D_1 + \frac{a}{b} D_x \right) & \left( \frac{11ab^2}{420} k_m^4 D_y - \frac{a}{5} k_m^2 D_{xy} - \frac{3a}{5} k_m^2 D_1 - \frac{3a}{b^2} D_x \right) & \left( \frac{ab^3}{210} k_m^4 D_y + \frac{4ab}{15} k_m^2 D_{xy} + \frac{2ab}{15} k_m^2 D_1 + \frac{2a}{b} D_x \right) \\ \left( -\frac{13ab^2}{840} k_m^4 D_y + \frac{a}{5} k_m^2 D_{xy} + \frac{3a}{10} k_m^2 D_1 + \frac{3a}{b^2} D_x \right) & \left( -\frac{ab}{30} k_m^2 D_1 + \frac{a}{b} D_x \right) & \left( -\frac{11ab^2}{420} k_m^4 D_y - \frac{a}{5} k_m^2 D_{xy} - \frac{3a}{5} k_m^2 D_1 - \frac{3a}{b^2} D_x \right) & \left( \frac{ab^3}{210} k_m^4 D_y + \frac{4ab}{15} k_m^2 D_{xy} + \frac{2ab}{15} k_m^2 D_1 + \frac{2a}{b} D_x \right) \end{bmatrix}$$

symmetric

where:  $k_m = \frac{m\pi}{a}$

Figure 2.4 Bending Initial Stiffness Matrix

$$[K_g] = C \begin{bmatrix}
 70(3T_1 + T_2) & 0 & 70(T_1 + T_2) & 0 & 0 & 0 & 0 & 0 \\
 70(3T_1 + T_2) & 70(3T_1 + T_2) & 0 & 70(T_1 + T_2) & 0 & 0 & 0 & 0 \\
 70(T_1 + T_2) & 0 & 70(T_1 + T_2) & 0 & 0 & 0 & 0 & 0 \\
 70(T_1 + 3T_2) & 70(T_1 + 3T_2) & 0 & 0 & 0 & 0 & 0 & 0 \\
 8(30T_1 + 9T_2) & 70(T_1 + 3T_2) & 0 & 0 & 0 & 0 & 0 & 0 \\
 2b(15T_1 + 7T_2) & 0 & 0 & 0 & 0 & 0 & 54(T_1 + T_2) & -2b(7T_1 + 6T_2) \\
 b^2(5T_1 + 3T_2) & 0 & 0 & 0 & 0 & 0 & 2b(6T_1 + 7T_2) & -3b^2(T_1 + T_2) \\
 24(3T_1 + 10T_2) & 0 & 0 & 0 & 0 & 0 & 24(3T_1 + 10T_2) & -2b(7T_1 + 15T_2) \\
 & & & & & & & b^2(3T_1 + 5T_2)
 \end{bmatrix}$$

*symmetric*

where:  $C = b(m\pi)^2 / 1680a$

Figure 2.5 Geometric Stiffness Matrix

### 2.2.2.2 Bending Initial Stiffness Matrix $[K_w\theta]$

The shape functions for use in determining the bending stiffness matrix are:

$$w = Y_m \left[ \left( 1 - \frac{3x^2}{b^2} + \frac{2x^3}{b^3} \right) \quad x \left( 1 - \frac{2x}{b} + \frac{x^2}{b^2} \right) \quad \left( \frac{3x^2}{b^2} - \frac{2x^3}{b^3} \right) \quad x \left( \frac{x^2}{b^2} - \frac{x}{b} \right) \right] \begin{Bmatrix} w_1 \\ \theta_1 \\ w_2 \\ \theta_2 \end{Bmatrix}$$

$$Y_m = \sin\left(\frac{m\pi y}{a}\right)$$

With the shape functions in this form, the strain-displacement matrix  $[B]$  can be written in terms of derivatives of  $[N]$ :

$$\{\varepsilon\} = \begin{Bmatrix} -\frac{\partial^2 w}{\partial x^2} \\ \frac{\partial^2 w}{\partial y^2} \\ \frac{\partial^2 w}{\partial x \partial y} \end{Bmatrix} = [B]\{d\} = [N']\{d\}$$

The explicit bending stiffness matrix for an element, or strip is given in Figure 2.4.

### 2.2.3 Geometric Stiffness Matrix for Plates

The geometric stiffness matrix for a plate strip subjected to linearly varying edge traction can be determined by either directly considering the higher order strain terms, or equivalently by forming the potential energy due to in-plane forces. The latter is the method selected for use here.

Consider a strip with linear edge traction as shown in Figure 2.6. The tractions correspond to linear edge stresses  $f_1$  and  $f_2$  via  $T_1 = f_1 t$  and  $T_2 = f_2 t$ .

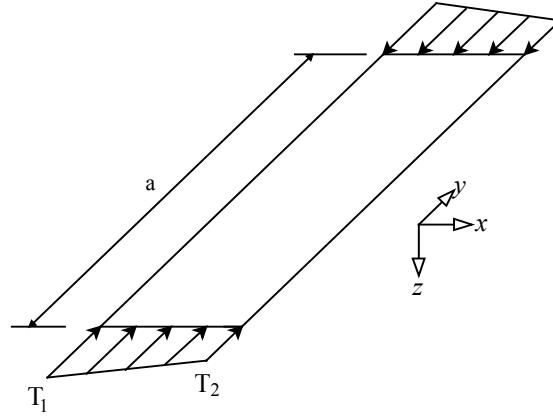


Figure 2.6 Strip with Edge Traction

The expression for the potential energy ( $U$ ) due to the in-plane forces is:

$$U = \frac{1}{2} \int_0^a \int_0^b \left( T_1 - (T_1 - T_2) \frac{x}{b} \right) \left( \left[ \frac{\partial u}{\partial y} \quad \frac{\partial v}{\partial y} \quad \frac{\partial w}{\partial y} \right] \left\{ \frac{\partial u}{\partial y} \quad \frac{\partial v}{\partial y} \quad \frac{\partial w}{\partial y} \right\}^T \right) dx dy$$

The derivatives in the expression for  $U$ , may be expressed in terms of the nodal degrees of freedom  $\{d\}$ . The matrix resulting from differentiating the shape functions in this case is called  $[G]$ .

$$\left\{ \frac{\partial u}{\partial y} \quad \frac{\partial v}{\partial y} \quad \frac{\partial w}{\partial y} \right\}^T = [G] \{d\}$$

The potential energy may now be expressed in terms of  $\{d\}$  and a matrix known as the geometric stiffness  $[K_g]$ .

$$U = \frac{1}{2} \{d\}^T [K_g] \{d\}$$

$$[K_g] = \int_0^a \int_0^b \left( T_1 - (T_1 - T_2) \frac{x}{b} \right) [G]^T [G] dx dy$$

The definition of  $[K_g]$  as a stiffness matrix follows directly from the energy derivation of an initial stiffness matrix (see Cook 1989 or Ugural and Fenster 1995 for energy derivation of an initial stiffness matrix, or Crisfield 1991 for more discussion of geometric stiffness matrices). For the problem at hand,  $[K_g]$  now takes the explicit form given in Figure 2.5.

### 2.2.4 Finite Strip Solution Methods

In the previous three sections explicit matrices are given for the initial stiffness and geometric stiffness of a discrete finite strip. For a member composed of multiple strips the contribution of each strip must be formed into a global initial stiffness and geometric stiffness. Thus:

$$[K] = \sum_{n=1}^{\#strips} [k]_n \quad \text{and} \quad [K_g] = \sum_{n=1}^{\#strips} [k_g]_n$$

The summation implies proper coordinate transformations and correct addition of the stiffness terms in the global coordinates and degrees of freedom. The elastic buckling problem is a standard eigenvalue problem of the following form:

$$[K]\{d\} = \lambda[K_g]\{d\}$$

Where the eigenvalues  $\lambda$ , are the buckling load, and the eigenvectors the buckling modes. Solution of such an eigenvalue problem may readily be solved in such programs as MATLAB (MathWorks Inc., 1996).

Both  $[K]$  and  $[K_g]$  are a function of the length,  $a$ . Therefore, the elastic buckling stress and the corresponding buckling modes are also a function of  $a$ . The problem can be solved for several lengths,  $a$ , and thus a complete picture of the elastic buckling stress and modes can be determined. The minima of such a curve could be considered as the critical buckling loads and modes for the member. The program CUSTRIP generates such curves, for more information on this program see the Appendix.

## 2.3 CLASSICAL SOLUTION: FOURIER SERIES METHOD FOR A SS PLATE

{section removed in this excerpt}

## 2.4 COMPARISON OF FINITE ELEMENT, FINITE STRIP, AND FOURIER SERIES SOLUTION

In the previous theoretical discussion of the finite element, finite strip, and Fourier Series methods little insight is given on qualitative interpretation of the results and direct comparison of the different methods. In order to address that issue two examples are examined. The first concerns a channel section with a longitudinal web stiffener in bending. The finite strip method and finite element method are compared and contrasted for this example. The second example consists of an isolated simply supported plate with a longitudinal stiffener in bending. All three methods are presented for this example, with particular emphasis given to the Fourier Series approach.

### 2.4.1 Example: Channel Section with a Longitudinal Web Stiffener

The selected problem is a C-section with a longitudinal web stiffener, under pure bending. The member geometry is from series of tests conducted at the University of Missouri-Rolla, the section label is B-1a-1. (Phung et. al. 1978). The inset of Figure 2.7 shows the geometry of the section. The observed failure mode is web-buckling and flange yielding.

#### 2.4.1.1 Finite Strip Analysis

A finite strip analysis is conducted on UMR section B-1a-1. The section is loaded under pure bending and analyzed at different lengths to determine the lowest buckling mode at each length. Figure 2.7 shows the section geometry and the finite strip analysis results. The curve shown in Figure 2.7 is typical of finite strip results. In this case, at half-wavelengths ( $\frac{1}{2}\lambda$ ) greater than approximately 65 in. lateral buckling occurs at a lower load than local web buckling.

The minima indicate the lowest load factor for a particular mode. Examining the finite strip results for half-wavelengths less than 65 inches, three distinct minima exist: local flange buckling at a  $\frac{1}{2}\lambda = 1.60''$ , and a load factor = 1.53 (i.e.,  $M_{cr} = 1.53M_y$ ); local web buckling at a  $\frac{1}{2}\lambda = 8.63''$  and a load factor = 0.69; and distortional Buckling at a  $\frac{1}{2}\lambda = 21.60''$  and a load factor = 0.71.

#### 2.4.1.2 Finite Element Analysis

##### FEM Comparison 1:

The elastic buckling finite element analysis is conducted using ABAQUS. The analysis consists of evaluating UMR B-1a-1 as simply supported at the end cross-sections, and unbraced over a length of 50 inches. Consistent nodal loads are derived for the end sections such that a pure bending moment equal to the yield moment is applied as a reference load.

Figure 2.9 - Figure 2.12 show the predicted buckling mode shapes for the three minima of the finite strip analysis. The results indicate that both the finite element analysis and finite strip analysis predict similar buckling load factors and mode shapes. Both methods report a minimum load factor/eigenvalue of 0.69 ( $M_{cr} = 0.69M_y$ ) consisting primarily of local web buckling. Both methods also report local flange buckling occurring at a minimum load factor/eigenvalue of 1.53.

Differences do exist between the finite element analysis results and the finite strip results. In Figure 2.11 the buckling mode from the finite element analysis at a load factor/eigenvalue of 1.33 is shown. In Figure 2.11 the mode shape in the compression flange is mixed between a longer wavelength distortional buckling and short wavelength local buckling in the compression flange. The result is that one distinct half-wavelength does not characterize this mode. Mixed wavelength modes are common in the finite element analysis but impossible in the given finite strip formulation.

##### FEM Comparison 2:

To further highlight the difference between the two methods, and in order to provide a more direct comparison between the finite element and finite strip buckling analysis, a second test is conducted. In this test the actual member length studied in the finite element analysis is varied.

This is similar to the method employed by the finite strip analysis for finding the first mode. Figure 2.8 shows the results for the two methods.

The curve shows the difference between analyzing the structure at different lengths and analyzing at different half-wavelengths. For instance, the lowest mode appears to require a larger physical length to develop than is indicated by the finite strip half-wavelength. In addition, the finite element analysis indicates that the lowest mode always decreases with the structure length - this is not so with the first mode half-wavelength curve of a finite strip analysis. The primary conclusion drawn from this analysis is the "up" part of a first mode half-wavelength curve should be considered fictitious. The lowest previous mode will still govern in the physical structure as the length is increased.

The box on the final point of the finite element curve of Figure 2.8 indicates the member length employed for FEM Comparison 1.

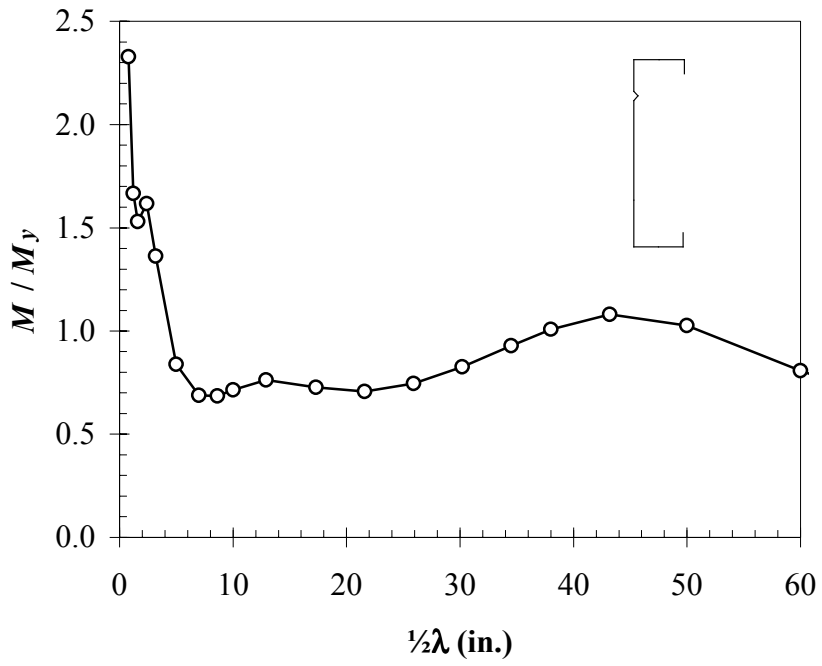


Figure 2.7 UMR B-1a-1 Finite Strip Results

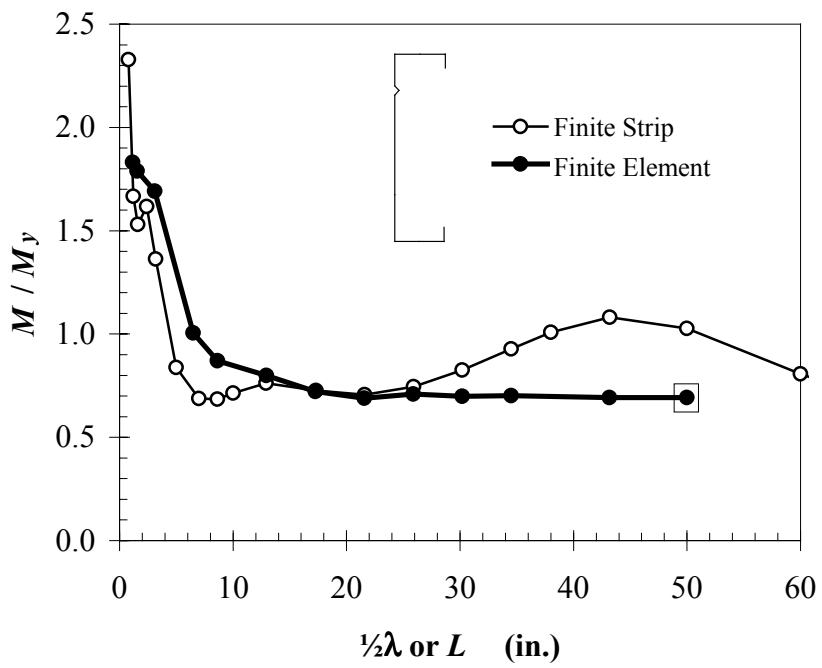
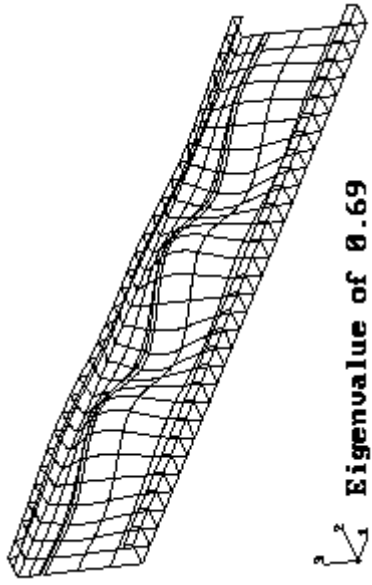
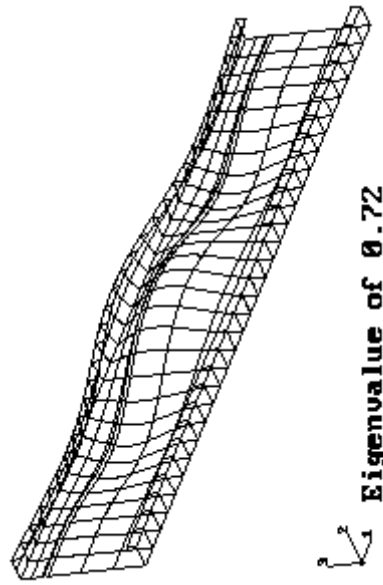


Figure 2.8 Direct Comparison of finite element and finite strip



*Figure 2.9 Local Web Buckling*



*Figure 2.10 Distortional Buckling*

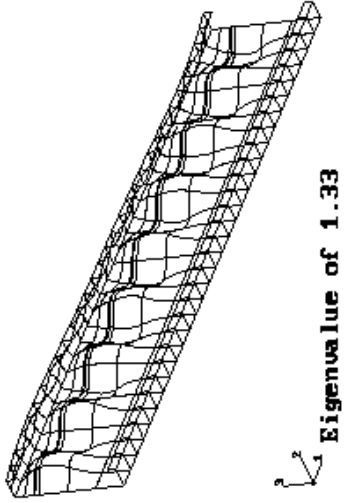


*Figure 2.11 Mixed-Mode Buckling*

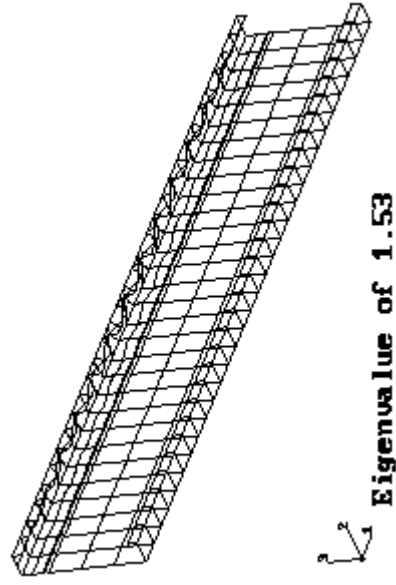


*Figure 2.12 Local Flange Buckling*

### 2.4.2 Example: SS Plate with a Longitudinal Stiffener in Pure Bending

In order to compare the results of the introduced analytical methods, and to understand better how to interpret the results an example problem has been selected for study by all three methods. The selected problem is shown in Figure 2.13. The loading is  $\xi = 2$ , or equal and opposite stresses.

For the Fourier analysis six transverse terms and 4 separate longitudinal sine terms are employed. The analysis is conducted using CUPLATE a program written in MATLAB, CUPLATE is discussed in the Appendix. The results are presented in a  $k$  vs.  $\beta$  or “buckling curve” as seen in Figure 2.14. The curves show that for small  $\beta$  (short plates) local buckling occurs. However as  $\beta$  increases the overall buckling of the plate controls. For reference, local buckling of a plate without a stiffener would result in a plate buckling coefficient ( $k$ ) of approximately 24.

The example problem may also be examined using finite strip and finite element techniques. The finite element solution is forced to mimic the methods used by the finite strip and Fourier Series solution by varying the length modeled and then plotting the first eigenmode for each length. In addition, the solutions for the buckling load are in terms of stress, or ratio of stress to  $f_y$ . These values are transformed into plate buckling coefficients. The finite strip solution, finite element solution using ABAQUS, and the minimum of the Fourier Series solution are all shown in Figure 2.15. A minimum curve similar to the Fourier Series could be generated using finite strip as well, but this is not done. Thus, the upwards branch of the finite strip curve after  $\beta > 1.5$  is not a cause for concern. All three methods yield minimum values within 5% of one another.

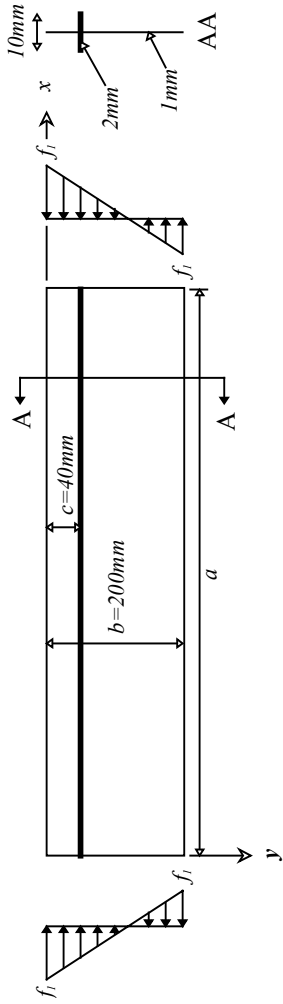


Figure 2.13 Geometry of Example Problem

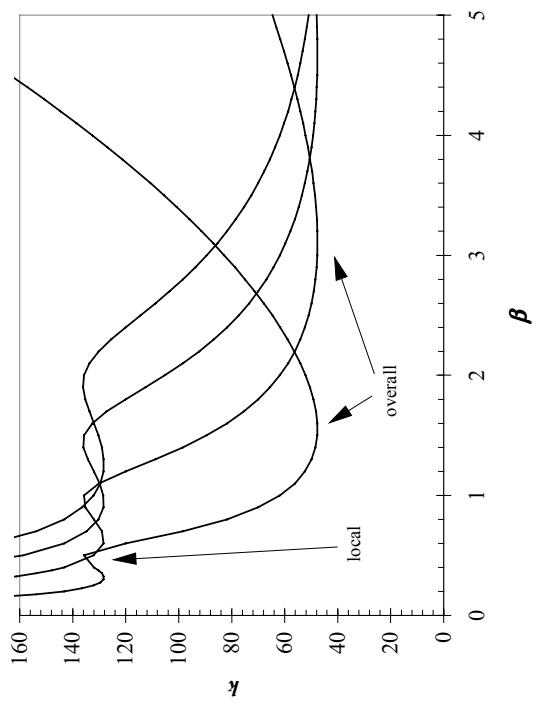


Figure 2.14 Fourier Analysis Solution

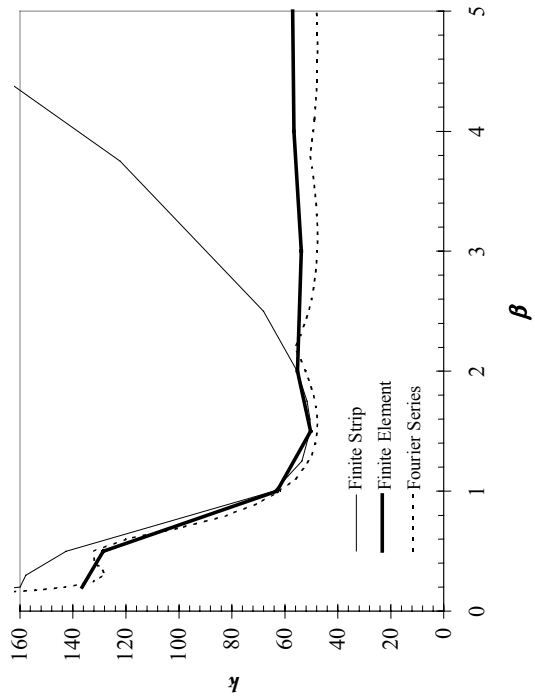


Figure 2.15 Comparison of Buckling Solutions

### **2.4.3 Conclusions and Comments about Comparison**

The primary conclusion of the two studied examples is that all three methods are adequate for characterizing the elastic buckling stress. However, the finite element implementation is the most robust of the three. The finite element procedure allows for varying support conditions at the ends and along the length. In addition, the geometry does not have to be regular along the length.

The finite strip implementation provides a useful tool for examining the behavior of cold-formed steel members. In particular, since the solution is efficient, parameter studies examining the elastic buckling stress proceed quickly. The finite strip method also properly accounts for the restraint between elements. As a result, it provides a way to examine the elastic buckling interaction of various elements, such as the web and flange of a bending member.

The classical Fourier Series solution only has limited use for solving general problems. As implemented it only applies for specialized boundary conditions. However, as a method for design it can be ideal. In particular, the method can be used to generate closed-form equations for the elastic buckling stress in special situations. It is in this capacity that its use is the most important.